

# RSC Advances



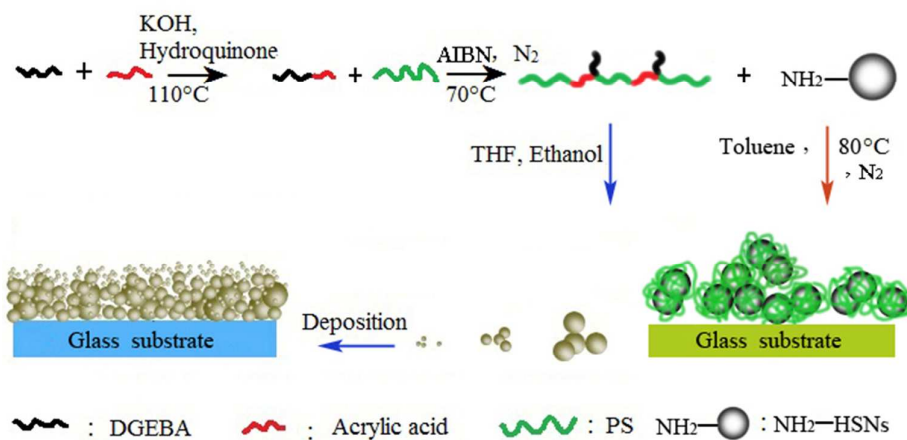
This is an *Accepted Manuscript*, which has been through the Royal Society of Chemistry peer review process and has been accepted for publication.

*Accepted Manuscripts* are published online shortly after acceptance, before technical editing, formatting and proof reading. Using this free service, authors can make their results available to the community, in citable form, before we publish the edited article. This *Accepted Manuscript* will be replaced by the edited, formatted and paginated article as soon as this is available.

You can find more information about *Accepted Manuscripts* in the [Information for Authors](#).

Please note that technical editing may introduce minor changes to the text and/or graphics, which may alter content. The journal's standard [Terms & Conditions](#) and the [Ethical guidelines](#) still apply. In no event shall the Royal Society of Chemistry be held responsible for any errors or omissions in this *Accepted Manuscript* or any consequences arising from the use of any information it contains.

**Abstract:** The copolymer of styrene and bisphenol A diglycidyl ether monoacrylate (PS-co-AADGEBAs) was synthesized by three steps from raw materials, and then it was used to fabricate a superhydrophobic surface via phase separation method. In particular the superhydrophobic surface not only exhibits superhydrophobicity to water and corrosive liquids, including acidic and basic solutions, but also shows good transparency, improved robustness and excellent aging resistance. Furthermore, the PS-co-AADGEBAs was also successfully grafted onto the surface of amino-functionalized hollow silica nanospheres (HSNs-NH<sub>2</sub>), then a (PS-co-AADGEBAs)-g-(HSNs-NH<sub>2</sub>) nanocomposite superhydrophobic surface was prepared. The obtained surfaces are promising materials for numerous potential applications fields, including electronics, biomedical, martial and defense-related areas.



## Design and fabrication of a novel superhydrophobic surface based on copolymer of styrene and bisphenol A diglycidyl ether monoacrylate

Jin-Qiu Liu<sup>a</sup>, Chong Bai<sup>a</sup>, De-Dong Jia<sup>a</sup>, Wei-Liang Liu<sup>a, \*</sup>, Fu-Yan He<sup>a</sup>, Qin-Ze Liu<sup>a</sup>, Jin-Shui Yao<sup>a</sup>, Xin-Qiang Wang<sup>b</sup>, Yong-Zhong Wu<sup>b</sup>

<sup>a</sup> *School of Materials Science and Engineering, Qilu University of Technology, Key Laboratory of Amorphous and Polycrystalline Materials, Key Laboratory of Processing and Testing Technology of Glass Functional Ceramics of Shandong Province, Jinan 250353, PR China*

<sup>b</sup> *State Key Laboratory of Crystal Materials, Shandong University, Jinan 250100, PR China*

\* Corresponding author: Wei-Liang LIU

Postal address:

Qilu University of Technology

School of Materials Science and Engineering

Daxue Road

Western University Science Park

Jinan, 250353

P. R. China

Tel: +86-531-89631227

Fax: +86-531-89631226

E-mail address: [wlliu@sdu.edu.cn](mailto:wlliu@sdu.edu.cn); [liuwl@qlu.edu.cn](mailto:liuwl@qlu.edu.cn)

**Abstract:** The copolymer of styrene and bisphenol A diglycidyl ether monoacrylate (PS-co-AADGEBAs) was synthesized by three steps from raw materials, and then it was used to fabricate a superhydrophobic surface via phase separation method. In particular the superhydrophobic surface not only exhibits superhydrophobicity to water and corrosive liquids, including acidic and basic solutions, but also shows good transparency, improved robustness and excellent aging resistance. Furthermore, the PS-co-AADGEBAs was also successfully grafted onto the surface of amino-functionalized hollow silica nanospheres (HSNs-NH<sub>2</sub>), then a (PS-co-AADGEBAs)-g-(HSNs-NH<sub>2</sub>) nanocomposite superhydrophobic surface was prepared. The obtained surfaces are promising materials for numerous potential applications fields, including electronics, biomedical, martial and defense-related areas.

**Keywords:** Superhydrophobic; High transmittance; Robustness; Copolymer; Hollow silica nanospheres;

## 1. Introduction

Surfaces with water contact angles (WCA) greater than  $150^\circ$  and sliding angles (SA) less than  $10^\circ$  are classified as superhydrophobic surfaces, which have attracted considerable interests over the past few decades. Generally, two strategies are adopted for the fabrication of superhydrophobic surfaces. That is, one is to roughen a low surface energy material, and the other is to make a rough substrate and modify it with low surface energy materials.<sup>1</sup> Various techniques, template/ hydrothermal method, self-assembly, chemical vapor deposition, electrochemical etching, and electrodeposition, have been used to fabricate superhydrophobic surfaces.<sup>2-12</sup> Meanwhile, different applications of which have been developed, for example, drag-reducing/ anti-icing/ anti-reflective surfaces, tunable wetting, microfluidic transportation, electroactive anticorrosive coatings and oil/water separation as well as reduction of bacterial adhesion.<sup>13-20</sup> However, the superhydrophobic surfaces generated via current surface modification techniques are mostly not suitable for practical applications due to limited mechanical robustness of surface structures.

Styrene (St) is the common low surface energy material in superhydrophobic area and easily acquired for practical application. Polymeric materials have been developed for the preparation of superhydrophobic surfaces, for instance the superhydrophobic surfaces prepared from a segmented polydimethylsiloxane-urea copolymer, a polyether based polyurethaneurea, poly(methyl methacrylate), polystyrene (PS), polycarbonate and a crosslinked epoxy resin are all discussed.<sup>21</sup> Superhydrophobic surfaces obtained by adding ethanol to the PS solution of tetrahydrofuran was ever reported by Zhiqing Yuan *et al.*<sup>22</sup> Shuaixia Tan *et al.* created brassica oleracea-like polymer surface using amorphous PS and demonstrated that the unitary micro-scale structure for a polymer surface can exhibit outstanding

water repellency as natural lotus.<sup>23</sup> In particular, PS based superhydrophobic films prepared by non-solvent induced phase separation method using tetrahydrofuran (THF) as the solvent and different alcohols as non-solvents were discussed,<sup>24</sup> A major problem of PS surfaces is that the poor resistance to mechanical abrasion. The adhesion of PS film to most substrates, especially polar substrates, is generally poor. A cast film of PS onto glass or silicon is easy to peel off, it could result in complete loss of the superhydrophobicity when immersed in water.<sup>25</sup>

Similarly, epoxy resin is one of the most important thermosetting polymers widely used as structural adhesives, coating, and composite materials due to its outstanding properties and great versatility.<sup>26</sup> Nonetheless, the water contact angle of the common epoxy resin is less than 90°, which is said to be hydrophilic.<sup>27</sup> Admittedly, the epoxy resin serves as an adhesion and stress relief layer, and the nanocomposite superhydrophobic surface showed improved mechanical robustness.<sup>28, 29</sup> Yang and co-workers consequently used polydimethylsiloxane as a negative template to cure the epoxy resin so as to obtain superhydrophobic surfaces with superior mechanical properties.<sup>30</sup>

In order to take advantage of adhesive property of epoxy resin and low surface energy of PS, we synthesized the copolymer of styrene and bisphenol A diglycidyl ether monoacrylate (PS-co-AADGEBA). Based on which, a transparent and robust polymeric superhydrophobic surface via phase separation method was created. Furthermore, the PS-co-AADGEBA was also successfully grafted onto the surfaces of amino-functionalized hollow silica nanospheres (HSNs-NH<sub>2</sub>), which was generated by a modified Stöber method.<sup>31</sup>

## 2. Experimental section

### 2.1. Materials

St was purified through vacuum distillation before used. The initiator azodiisobutyronitrile (AIBN) was purified by recrystallization from absolute ethanol. Bisphenol A, epichlorohydrin (EPI), sodium hydroxide (NaOH), acrylic acid (AA), potassium hydroxide (KOH), hydroquinone, toluene, THF, tetraethyl orthosilicate (TEOS), polyacrylic acid (PAA, Molecular weight of 3000), ammonia hydroxide (28 wt%), 3 - aminopropyl triethoxysilane (APTES), Na<sub>2</sub>SO<sub>4</sub>, ethyl acetate, petroleum ether, dichloromethane, ethanol, acetone and distilled water were used as received.

## 2.2. Synthesis of bisphenol A diglycidyl ether (DGEBA)

The synthesis of DGEBA is described in Scheme 1. A mixture of Bisphenol A (5.7 g), EPI (9.25 g) and NaOH solution (10 M, 10 ml) was stirred in a flask at 70~80 °C for 12 h. After confirming the complete conversion of the Bisphenol A and the intermediate by TLC, distilled water (15 ml) and toluene (30 ml) were added into the residue under vigorous stirring. The organic layer was separated, and washed by water to neutral. Afterward, it was dried over Na<sub>2</sub>SO<sub>4</sub> and concentrated in vacuo to give the crude product, which was purified by column chromatography (ethyl acetate /petroleum ether = 1/3) to provide DGEBA as a viscous, transparent liquid.

## 2.3. Synthesis of bisphenol A diglycidyl ether monoacrylate (AADGEBA)

The KOH (0.03 g) was dissolved in AA (0.75 g), and then the solution was added to the mixture composed of DGEBA (3.92 g), hydroquinone (0.37 g) and toluene (80 mL). The reaction was carried out at 90~110 °C for 4~7 h. Confirming the complete conversion of the DGEBA by TLC, afterward similar treatments were performed as those of DGEBA preparation, then AADGEBA could be obtained as a slightly yellow, transparent liquid. The synthesis process of AADGEBA is summarized in Scheme 2.

## 2.4. Synthesis of PS-co-AADGEBA

The synthesis of PS-co-AADGEBA is expressed in Scheme 3. Free-radical

copolymerization of St and AADGEBa was performed at 70 °C in THF at nitrogen atmosphere using AIBN as the initiator. After 48 h polymerization, copolymers of St and AADGEBa were precipitated by ethanol and water (volume ratio of 2:8). The precipitates were dissolved in acetone and reprecipitated by ethanol and water for three times. Subsequently, the products were dried in a vacuum oven at 30 °C for 24 h.

#### 2.5. Fabrication of the PS-co-AADGEBa surface

The PS-co-AADGEBa (0.10 g) was dissolved in THF (4ml) at the refluxed temperature under stirring. Afterwards, the pure ethanol was added into the solution. The glass substrates were washed by using an ultrasonic generator for 30 min in ethanol to remove the dust and dried in the air. A particulate film was thereupon developed by dispensing 0.5 ml of the dispersion onto a cleaned glass substrate of 2×2 cm and evaporating the solvent at room temperature. Meanwhile, the smooth copolymer surface as a reference was prepared by directly dropping the copolymer/THF solution onto the cleaned glass substrate without adding any ethanol.

#### 2.6. Characterization

Bruker VERTEX-70 Fourier transform infrared (FTIR) spectrometer was used to investigate the DGEBA, AADGEBa and PS-co-AADGEBa. H-nuclear magnetic resonance (<sup>1</sup>H NMR) spectra of DGEBA, AADGEBa and PS-co-AADGEBa were obtained on a Bruker AVANCE11400 spectrometer in CDCl<sub>3</sub> at room temperature. Molecular weights and molecular weight polydispersities (M<sub>w</sub>/M<sub>n</sub>) of the copolymers were determined with a DAWN HELEOS multiangle laser light scattering (MALLS) detector. Thermogravimetric (TG) analyses were performed using a STA-449C apparatus. The samples were heated from room temperature to 800 °C at a heating rate of 10 °C/min under nitrogen purge. The glass transition temperatures (T<sub>g</sub>) of



polymers were measured by a TAQ10 differential scanning calorimeter (DSC). The measurements were performed from 60 to 140 °C at a heating rate of 10 °C/min under nitrogen purge. The morphologies of the prepared surfaces were observed by scanning electron microscopy (SEM, Hitachi S-4800, Japan) at an accelerating voltage of 5 kV, and the WCA and SA were measured on contact angle tester SL200B (Solon Technology Science Co., Ltd) at ambient temperature with about 5  $\mu$ L liquid droplets.

### 3. Results and discussion

#### 3.1. Characterization of DGEBA, AADGEBA and PS-co-AADGEBA

##### 3.1.1. FTIR spectra of DGEBA, AADGEBA and PS-co-AADGEBA

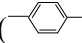
The structures of DGEBA, AADGEBA and PS-co-AADGEBA were characterized by FTIR. As shown in Fig. 1 a, the characteristic absorptions of bisphenol A appear at 2964  $\text{cm}^{-1}$  ( $\nu_s$ ,  $\text{CH}_3$ ) and 2869  $\text{cm}^{-1}$  ( $\nu_a$ ,  $\text{CH}_3$ ) in the C-H stretching region, respectively. The peaks at 1608, 1512 and 1455  $\text{cm}^{-1}$  are the typical absorption of the C=C bond on the benzene ring, while the presence of aromatic ether bond and fatty ether bond (C-O) stretching vibration of DGEBA is supported by the absorptions around 1251 and 1035  $\text{cm}^{-1}$ . The peak at 1302  $\text{cm}^{-1}$ , corresponds to the stretch mode of C-C bond, and the one at 832  $\text{cm}^{-1}$  is C-H bending vibration of multi-substituted phenyl ring.<sup>32</sup> To sum up, the appearance of the above signals indicates the formation of DGEBA.

Figure 1 b shows characteristic absorptions of C=O, C=C appeared at 1728 and 1640  $\text{cm}^{-1}$ .<sup>33</sup> The absorption of fatty ether bond (C-O) at 1035  $\text{cm}^{-1}$  is significantly reduced, and the amplitude at 3460  $\text{cm}^{-1}$  stretching vibration absorption of O-H emerge clearly.

In Fig. 1 c, the typical absorption of the monosubstituted benzene ring is supported by the amplitudes around 755 and 697  $\text{cm}^{-1}$ , and five sharp peaks around 3000  $\text{cm}^{-1}$  are the characteristic absorptions of polystyrene.<sup>34</sup> At the same time, the signal at

1640  $\text{cm}^{-1}$  disappears, demonstrating that the PS-co-AADGEBA has been acquired.

### 3.1.2. $^1\text{H}$ NMR spectra of DGEBA, AADGEBA and PS-co-AADGEBA

$^1\text{H}$  NMR spectra of DGEBA, AADGEBA and PS-co-AADGEBA were obtained in  $\text{CDCl}_3$  at room temperature, as shown in Fig. 2. The  $^1\text{H}$  NMR spectrum in Fig. 2 a have characteristic shift signals of DGEBA ( $\delta = 7.14, 6.83, 4.26\sim 2.70, 1.64$  ppm). Assignments of these peaks are as follows: at 7.14 and 6.83 ppm to proton signals on the benzene ring () , at 4.26~2.70 ppm to the saturated proton signals ( $-\overset{|}{\text{C}}\text{H}-$ ,  $-\text{CH}_2-$ ), and at 1.64 ppm to the saturated proton signals ( $-\text{CH}_3$ ). The  $^1\text{H}$  NMR spectrum of AADGEBA based on DGEBA is represented in Fig. 2 b. The  $^1\text{H}$  NMR spectra of DGEBA and AADGEBA are found to be typical to each other except the presence of signals at 5.85~6.55, and 2.06 ppm, corresponding to the protons of acrylate ( $\text{CH}_2=\overset{|}{\text{C}}\text{H}-$ ) and hydroxyl groups ( $-\text{OH}$ ), respectively. The emergence of hydroxyl proton signals proves the occurrence of ring-opening reaction of acrylic acid and DGEBA. The  $^1\text{H}$  NMR spectrum in Fig. 2 c has characteristic shift signals of PS ( $\delta = 7.47\sim 6.24, 2.33\sim 0.79$  ppm) and AADGEBA ( $\delta = 4.23\sim 2.70, 2.33\sim 0.79$  ppm), while proton signals at 5.85~6.55 ppm disappear, which demonstrate the successful copolymerization of PS and AADGEBA (See also the details on  $^1\text{H}$  NMR spectra of DGEBA, AADGEBA and PS-co-AADGEBA in the Supporting Information).

### 3.1.3. DSC curves of PS and PS-co-AADGEBA

The DSC curves of PS and PS-co-AADGEBA are shown in Fig. 3. The glass transition temperature ( $T_g$ ) values of PS-co-AADGEBA (Fig. 3 a) is close to 80  $^\circ\text{C}$ , lower than that of pure PS (Fig. 3 b), which is approaching 98  $^\circ\text{C}$ . After the polymerization of PS and AADGEBA, the number of benzene rings on the polymer chain reduces, enriching the flexibility of the polymer chain, so the  $T_g$  values

decreases correspondingly. In addition, DSC measurements showed that both of them exhibit single glass transition temperature, indicating that the products are the single substance but blends.

#### 3.1.4 GPC analysis of PS-co-AADGEBAs

Figure 4 shows the GPC curves of PS-co-AADGEBAs. The weighted-average molar mass ( $M_w$ ) and the number-average molecular weight ( $M_n$ ) of PS-co-AADGEBAs, measured from MALLS, are about  $1.421 \times 10^4$  and  $1.195 \times 10^4$  g/mol, respectively. So a fairly narrow molecular weight distribution,  $M_w/M_n = 1.189$ , were obtained.

In summary, all of the experimental results are coincident, illustrating that the target copolymers has been obtained.

### 3.2. Characterization of surface morphology

#### 3.2.1 SEM images of the PS-co-AADGEBAs surface

When the solution of the copolymer/THF dried under ambient temperature on the glass substrate by drop coating, the WCA of the surface was measured to be  $93.4^\circ$  (Fig. 5 a). With increasing volume fraction of ethanol, the degree of copolymer phase separation increased, resulting in the formation of rough surfaces (Fig. 5 b). The variation of contact angles of these surfaces is shown in Fig. 6. It is evident that the maximum contact angle is  $155.2^\circ$  and the best content of ethanol is about 50%. The surface prepared from the copolymer solution with THF (50%) as solvent consists of numerous micron-sized particles (Fig. 5 c), and the large particles are about ten times the size of the small particles. The investigations indubitably revealed that the surface was superhydrophobic, possessing water contact angles of  $\sim 155.2^\circ$  and water sliding angles of  $\sim 4^\circ$ .

#### 3.2.2 Analysis of the surface morphology

The possible formation mechanism of the PS-co-AADGEBAs surface can be

described as follows (Fig. 7). Phase separation and self-assembly of amphiphilic PS-co-AADGEBAs worked simultaneously, which was a spontaneous process. In the beginning, the linear chains of PS-co-AADGEBAs stretched freely in copolymer solution, along with the evaporation of solvent, the stretching PS-co-AADGEBAs chains in the solution self-assembled into spherical coils, then aggregated to small particles with the groups of hydrophilic inside and the ones of hydrophobic outside.<sup>35</sup> In order to reduce the surface energy further, some spherical particles will reunite to form bigger particles and the small ones will attach themselves to the surfaces of the bigger ones.

Analysis of solvent parameters, rapid solvent evaporation should produce a percolated polymer network, and slower evaporation should be conducive to discrete particle formation. The evaporation rate of ethanol (see Table 1) is lower than THF, and the two solvents successively acted in forming micro-particles. The differences in solubility parameters (9.5 and 11.3 MPa<sup>1/2</sup>) for the two solvents indicate that the mixture was more polar and should be a better solvent for the AADGEBAs. The polar and hydrogen-bonding components of the solubility parameter of ethanol are considerably larger than those from THF (see Table 1), which suggests that the ethanol will preferentially interact, or solvate, the polar segments, which will decrease the dipolar interactions of the copolymer in solution and expand the polymer chain.<sup>25</sup>

To better understand the superhydrophobic property of the prepared surface thoroughly, we verified the classical theory of superhydrophobic surface on it. When a droplet placed on a smooth surface, the intrinsic contact angle named Young's contact angle ( $\theta$ ) is given by the relative surface energies of the solid-liquid ( $\gamma_{SL}$ ), solid-air ( $\gamma_{SA}$ ), and liquid-air ( $\gamma_{LA}$ ) interfaces as<sup>36</sup>

$$\theta = \cos^{-1} \left( \frac{\gamma_{SA} - \gamma_{SL}}{\gamma_{LA}} \right) \quad (1)$$

Wenzel proposed a model,<sup>37</sup> shown in Eq. 2 to describe the wettability on a surface,

$$\cos \theta_r = r \cos \theta \quad (2)$$

Here,  $r$  is the roughness factor, and  $\theta$  and  $\theta_r$  are the equilibrium contact angles of a liquid on a smooth solid surface and a rough solid surface, respectively. According to Eq. 2, if the roughness is increased, the contact angle of a hydrophobic solid surface will increase also. The WCA of the surface of copolymer/THF solution was measured 93.4°, which is an intrinsic hydrophobic surface. Thus, according to the Wenzel model, we believe that the rough surfaces observed in SEM by phase separation should be more hydrophobic than the smooth one. The WCA of the surface of copolymer/THF (50%) as solvent was measured 155.2°, which was consistent with the theory.

On the other hand, a droplet gently deposited on a rough surface that favors the Cassie state energetically stays in the Cassie state with a high contact angle as given by<sup>38</sup>

$$\theta_r = \cos^{-1} (-1 + \phi(1 + \cos \theta)) \quad (3)$$

Here  $\theta_r$  is the WCA of the PS-co-AADGEBa superhydrophobic surface, while  $\theta$  is the equilibrium WCA on the smooth PS-co-AADGEBa surface and  $\phi$  is the solid area fraction defined as the ratio of the projected area to the base area of the surface. Based on the WCA data that were obtained ( $\theta = 93.4^\circ$  and  $\theta_r = 155.2^\circ$ ), the value of  $\phi$  is calculated about 0.098 (<1). These results are responsible for the superhydrophobic property.

### 3.3. Feature and characterization of surface property

With the epoxy group in side chain, the copolymer possesses certainly adhesive properties, hence the mechanical robustness of the superhydrophobic surface should be improved. In the following paragraph, the corrosion and aging resistance, the transparency and the mechanical robustness of the surface have been examined to verify the speculation.

#### 3.3.1. Corrosion and aging resistance evaluation

The wettability of different liquids with pH values of 3 to 10 on the PS-co-AADGEBAs surface was studied. Strong acid and alkaline liquid droplets contact angles are all above  $150^\circ$  as shown in Fig. 8 a, which illustrated that the surface we prepared possesses superhydrophobic properties not only for pure water but also for corrosive liquids. The result is very attractive for applications in corrosive environments.

As shown in Fig. 8 c, the aging tests for the PS-co-AADGEBAs superhydrophobic surface were also conducted. The surface was exposed indoor for 140 days at room temperature. The water contact angles are still greater than  $150^\circ$ , notwithstanding decrease a little, revealing excellent aging resistance for the PS-co-AADGEBAs superhydrophobic surface.

#### 3.3.2. Transparency and mechanical robustness test

Recently, more and more attention has been focused on creating coatings with both superhydrophobic and transparent properties.<sup>39</sup> In this paper, a solution of the PS-co-AADGEBAs nanoparticles obtained via phase separation was dip-coated on the

surfaces of cleaned glass substrates. The transparency of the surface was directly visible and the mechanical property of the surface was observed by impact of water.

As a result, the PS-co-AADGEBAsuperhydrophobic surface shows high light transmittance, which is visible in Fig. 9 a and b. Acid and alkali droplets indicate superhydrophobicity with methyl orange and phenolphthalein indicator, respectively. Moreover, it is also stable for hot water as hot as 50 °C, as shown in Fig. 9 c. In order to investigate the stability of the superhydrophobic surface against the impact of water, experiments were conducted by impinging the surface under running water. The surface, which can be seen via the video in the supporting materials, emerges good adhesion to the glass substrate and remains integrated and superhydrophobic. It can be interpreted that a hydrogen bond generates when particles of PS-co-AADGEBAland on the glass substrate, and the hydroxyls of epoxy resin and the rich hydroxyls from the glass substrate tend to combine together owing to the van der Waals interaction.<sup>40</sup>

### 3.4 Application of the copolymer

The PS-co-AADGEBAs was also successfully grafted onto the surfaces of amino-functionalized hollow silica nanospheres (HSNs-NH<sub>2</sub>), then a (PS-co-AADGEBAs)-g-(HSNs-NH<sub>2</sub>) nanocomposite superhydrophobic surface was prepared through casting drops of (PS-co-AADGEBAs)-g-(HSNs-NH<sub>2</sub>)/toluene on the cleaned glass substrate (the details seen also in the Supporting Information).

To confirm the presence of amino groups on the surface of HSN<sub>s</sub>, FTIR spectra of HSNs-NH<sub>2</sub> were investigated by using the pure HSNs as reference (Fig. 10 a and b). The transmission bands at 2920, 2850cm<sup>-1</sup> assign to the asymmetric ( $\nu_{as}$ ) stretching vibrations of methylene (CH<sub>2</sub>) from the hydrolysis and condensation of -Si-(CH<sub>2</sub>)<sub>3</sub>-NH<sub>2</sub> of APTES. The typical absorption of the monosubstituted benzene ring is

supported by the peaks around 755 and 697  $\text{cm}^{-1}$ , and peaks around 3000  $\text{cm}^{-1}$  are the characteristic absorptions of polystyrene (Fig. 10 c).

Figure 11 shows TG curves of HSNs-NH<sub>2</sub> and (PS-co-AADGEBEBA)-g-(HSNs-NH<sub>2</sub>). The silica remain stable up to about 800 °C. The decomposition temperature at maximum rate ( $T_{\text{peak}}$ ) for (PS-co-AADGEBEBA)-g-(HSNs-NH<sub>2</sub>) is approaching 350 °C, which is accordant with the degradation of PS and DGEBA.<sup>41</sup> Accordingly, these results indicate that a 11.5% and a 26.5% loss were observed for HSNs-NH<sub>2</sub> and (PS-co-AADGEBEBA)-g-(HSNs-NH<sub>2</sub>), respectively.

SEM images of the (PS-co-AADGEBEBA)-g-(HSNs-NH<sub>2</sub>) surface are shown in Fig. 5 d, rough structures of (PS-co-AADGEBEBA)-g-(HSNs-NH<sub>2</sub>) and its aggregates guarantee a large amount of air can be trapped at the surface, which is beneficial for water droplets roll on it. The investigations showed that the (PS-co-AADGEBEBA)-g-(HSNs-NH<sub>2</sub>) surface was superhydrophobic, possessing water contact angles of  $\sim 158.6^\circ$ , and water sliding angles of  $\sim 3^\circ$ .

The superhydrophobic surface created with (PS-co-AADGEBEBA)-g-(HSNs-NH<sub>2</sub>) shows ideal corrosion and aging resistance, as shown in Fig. 8 b and d. But it has poor transparency and weak resistance to the impact of water. Subsequent effort should be focused on the transparency and mechanical robustness of the nanocomposite superhydrophobic surface. The transparency of HSNs superhydrophobic surface has been reported by Ligang Xu.<sup>42</sup> It is possible that the presence of epoxy groups in the (PS-co-AADGEBEBA)-g-(HSNs-NH<sub>2</sub>), and hence studies on the curing of (PS-co-AADGEBEBA)-g-(HSNs-NH<sub>2</sub>) with epoxy curing agents is essential.

#### 4. Conclusions

In summary, the copolymer of styrene and bisphenol A diglycidyl ether monoacrylate (PS-co-AADGEBEBA) was synthesized. The novel polymeric



superhydrophobic and a nanocomposite superhydrophobic surface were fabricated based on the copolymer. The polymeric surface was transparent and exhibited improved mechanical robustness due to the presence of the epoxy resin in the copolymer. Both the surfaces showed attractive stability for corrosive liquids and excellent aging resistance to withstand real world applications.

#### Acknowledgements

This work is supported by Shandong Province Natural Science Foundation (ZR2012EMM009 and ZR2013EMQ005), the Scientific Research Foundation for the Returned Overseas Scholars in Jinan (20100406), National Natural Science Foundations of China (51372140, 51303086 and 51172132), the Youth Scientist Funds of Shandong Province (BS2011CL025).

## References

- 1 V.A. Ganesh, H.K. Raut, A.S. Nair and S. Ramakrishna, *J. Mater. Chem.*, 2011, **21**, 16304.
- 2 Y. Rahmawan, L.B Xu and S. Yang, *J. Mater. Chem. A*, 2013, **1**, 2955.
- 3 C.R. Crick, J.C. Bear, P. Southern and I.P. Parkin, *J. Mater. Chem. A*, 2013, **1**, 4336.
- 4 Q.F. Xu, B. Mondal and A.M. Lyons, *ACS Appl. Mater. Inter.*, 2011, **3**, 3508.
- 5 Y. Lu, J.L. Song, X. Liu, W.J. Xu, Y.J. Xing and Z.F. Wei, *ACS Sustainable Chem. Eng.*, 2013, **1**, 102.
- 6 H. Ogihara, J. Xie, J. Okagaki and T. Saji, *Langmuir*, 2012, **28**, 4605.
- 7 Z. Chen, L.M. Hao and C. Chen, *Colloid Surf. A-Physicochem. Eng. Asp.*, 2012, **401**, 1.
- 8 S.L. Wang, C.Y. Wang, C.Y. Liu, M. Zhang, H. Ma and J. Li, *Colloid Surf. A-Physicochem. Eng. Asp.*, 2012, **403**, 29.
- 9 Z.G. Guo, W.M. Liu and B-L. Su, *J. Colloid Inter. Sci.*, 2011, **353**, 335.
- 10 E. Celia, T. Darmanin, E. Taffin de Givenchy, S. Amigoni and F. Guittard, *J. Colloid Inter. Sci.*, 2013, **402**, 1.
- 11 X.D. Tang, S.Q. Nan, T.S. Wang, Y. Chen, F.Q. Yu, G.Z. Zhang and M.S. Pei, *RSC Adv.*, 2013, **3**, 15571.
- 12 S.H. Liu, M. Sakai, B.S. Liu, C. Terashima, K. Nakata and A. Fujishima, *RSC Adv.*, 2013, **3**, 22825.
- 13 Y.Y. Wang, J. Xue, Q.J. Wang, Q.M. Chen and J.F. Ding, *ACS Appl. Mater. Inter.*, 2013, **5**, 853.
- 14 A. Yildirim, T. Khudiyev, B. Daglar, H. Budunoglu, A.K. Okyay and M. Bayindir, *ACS Appl. Mater. Inter.*, 2013, **5**, 853.
- 15 E. Ueda and P.A. Levkin, *Adv. Mater.*, 2013, **25**, 1234.
- 16 S.Y. Xing, J. Jiang and T.R. Pan, *Lab on a Chip*, 2013, **13**, 1937.
- 17 H.Y. Dong, M.J. Cheng, Y.J. Zhang, H. Wei and F. Shi, *J. Mater. Chem. A*, 2013, **1**, 5886.
- 18 K-C. Chang, H-I Lu, C-W Peng, M-C. Lai, S-C Hsu, M-H Hsu, Y-K Tsai, C-H Chang, W-I Hung, Y. Wei and J-M Yeh, *ACS Appl. Mater. Inter.*, 2013, **5**, 1460.

- 19 X.X. Zhang, L. Wang and E. Levänen, *RSC Adv.*, 2013, **3**, 12003.
- 20 J.L. Yong, Q. Yang, F. Chen, D.S. Zhang, G.Q. Du, H. Bian, J.H. Si and X. Hou, *RSC Adv.*, 2014, **4**, 8138.
- 21 I. Yilgor, S. Bilgin, M. Isik and E. Yilgor, *Polymer*, 2012, **53**, 1180.
- 22 Z.Q. Yuan, H. Chen, J.X. Tang, X. Chen, D.J. Zhao and Z.X. Wang, *Surf. Coat. Tech.*, 2007, 201, 7138.
- 23 S.X. Tan, Q.D. Xie, X.Y. Lu, N. Zhao, X.L. Zhang and J. Xu, *J. Colloid. Interf. Sci.*, 2008, 322, 1.
- 24 S.T. Aruna, P.Binsy, R. Edna and J.B. Bharathibai, *Appl. Surf. Sci.*, 2012, **258**, 3202.
- 25 X.Y. Wang and R.A. Weiss, *Langmuir*, 2012, 28, 3298.
- 26 S.H. Mansour, N. Mostafa and L. Abd-El-Messieh, *Eur. Polym. J.*, 2007, **43**, 4770.
- 27 C.Q. Wang, J.Y. Xiao, J.C. Zeng, D.Z. Jiang and Z.Q. Yuan, *Mater. Chem. Phys.*, 2012, **135**, 10.
- 28 Y. Liu, Z.Y. Lin, W. Lin, K.S. Moon and C.P. Wong, *ACS Appl. Mater. Inter.*, 2012, **4**, 3959.
- 29 Y.H. Xiu, Y. Liu, B. Balu, D. W. Hess and C.P. Wong, *IEEE T COMP PACK MAN*, 2012, **2**, 395.
- 30 T-I Yang, C-W Peng, Y.L. Lin, C-J Weng, G. Edgington, A. Mylonakis, T-C Huang, C-H Hsu, J-M Yeh and Y. Wei, *J. Mater. Chem.*, 2012, **22**, 15845.
- 31 Y. Wan and S-H Yu, *J. Phys. Chem. C*, 2008, **112**, 3641.
- 32 M. ABBATE, E. MARTUSCELLI, P. MUSTO, G. RACOSTA and G. SCARINZI, *J. Polym. Sci. Pol. Phys.*, 1994, **32**, 395.
- 33 B. Zhong, D.B. Chen, Z.H. Zhou, A.Y. Zhong and Z.Y. Du, *J. Appl. Polym. Sci.*, 1998, **69**, 1855.
- 34 H. Fallahi and G.A. Koohmarch, *J. Appl. Polym. Sci.*, 2013, **127**, 523.
- 35 J.T. Zhu and W. Jiang, *Mater. Chem. Phys.*, 2007, **101**, 56.
- 36 S. Dash, M.T. Alt, S.V. Garimella, *Langmuir*, 2012, **28**, 9606.
- 37 R.N. Wenzel, *Ind. Eng. Chem.*, 1936, **28**, 988.
- 38 N.A. Patankar, *Langmuir*, 2004, **20**, 7097.

- 39 G.Y. Wang, H.R. Wang, Z.G. Guo, *Chem. Commun.*, 2013, **49**, 7310.
- 40 Y.F. Li, H.Q. Yu, H. Li, C.G. An, K. Zhang, K.M. Liew and X.F. Liu, *J. Phys. Chem. C*, 2011, **115**, 6229.
- 41 H. Feng, X.D. Wang, D.Z. Wu, *Ind. Eng. Chem. Res.*, 2013, **52**, 10160.
- 42 L.G. Xu and J.H. He, *Langmuir*, 2012, **28**, 7512.

## Captions for Figures and Schemes

Table 1. Solvent parameters

Fig. 1. FTIR spectra of (a) DGEBA (b) AADGEBA (c) PS-co-AADGEBA.

Fig. 2.  $^1\text{H}$  NMR spectra of (a) DGEBA (b) AADGEBA (c) PS-co-AADGEBA.

Fig. 3. DSC curves of (a) PS-co-AADGEBA (b) PS.

Fig. 4. GPC curves of PS-co-AADGEBA.

Fig. 5. SEM images of the PS-co-AADGEBA surface with different ethanol contents in the copolymer/THF solution: (a) 0%; (b) 30%; (c) 50%; (d) the (PS-co-AADGEBA)-g-(HSNs-NH<sub>2</sub>) surface.

Fig. 6. The variation of water contact angles of the PS-co-AADGEBA surface with different ethanol contents.

Fig. 7. Schematic diagram for the formation of the PS-co-AADGEBA surface.

Fig. 8. CA as a function of pH value and exposure time for the PS-co-AADGEBA surface (a, c) and the (PS-co-AADGEBA)-g-(HSNs-NH<sub>2</sub>) surface (b, d), respectively.

Fig. 9. Acid and alkali droplets on the PS-co-AADGEBA surface (a) acid droplets with methyl orange indicator (b) alkali droplets with phenolphthalein indicator (c) hot water of 50°C.

Fig. 10. FTIR spectra of (a) HSNs (b) HSNs-NH<sub>2</sub> (c) (PS-co-AADGEBA)-g-(HSNs-NH<sub>2</sub>).

Fig. 11. TG curves of (a) HSNs-NH<sub>2</sub> (b) (PS-co-AADGEBA)-g-(HSNs-NH<sub>2</sub>).

Scheme 1. Synthesis of DGEBA.

Scheme 2. Synthesis of AADGEBA.

Scheme 3. Synthesis of PS-co-AADGEBA.

**Table 1. Solvent parameters**

Solvent	Evaporation rate (N-BAC=1)	Hansen, Solubility Parameters (MPa <sup>1/2</sup> )			
		Total	Nonpolar	Polar	Hydrogen Bonding
THF	6.3	9.5	8.2	2.8	3.9
Ethanol	1.7-1.9	13	7.7	4.3	9.5
THF/ ethanol(v/v=1/1)	-	11.3	8	3.6	6.7

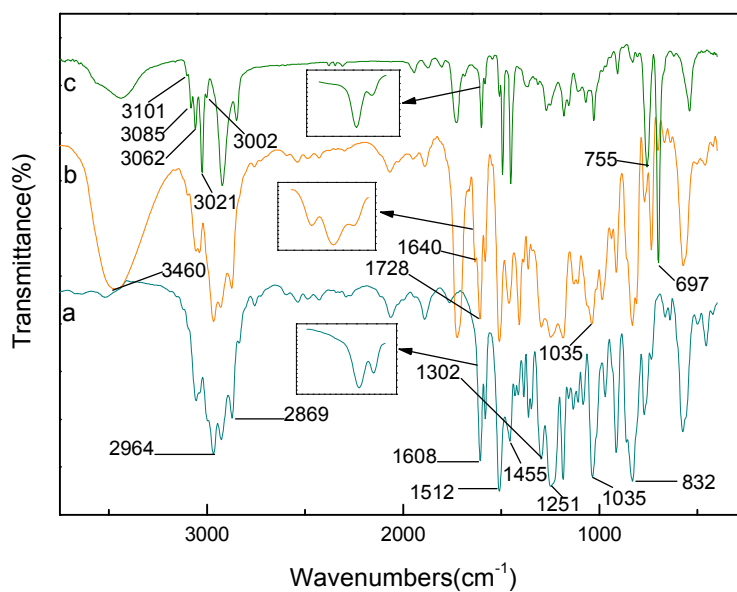


Fig. 1. FTIR spectra of (a) DGEBA (b) AADGEBA (c) PS-co-AADGEBA.

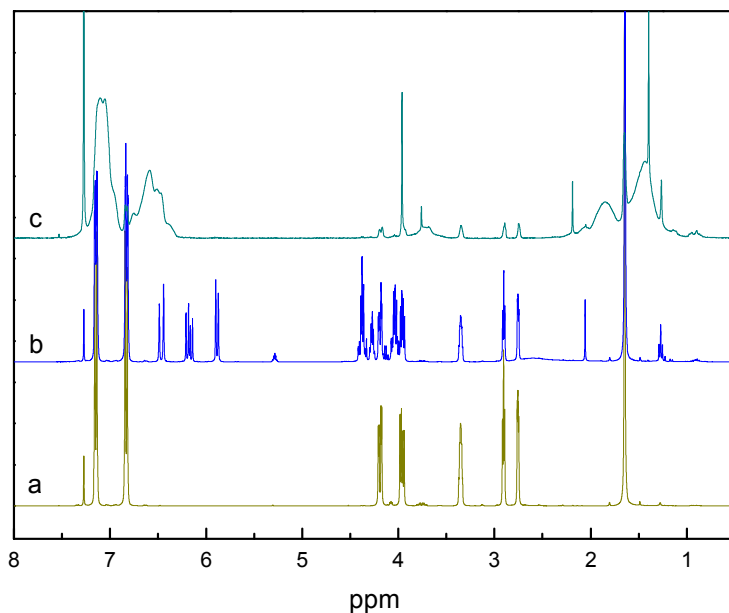
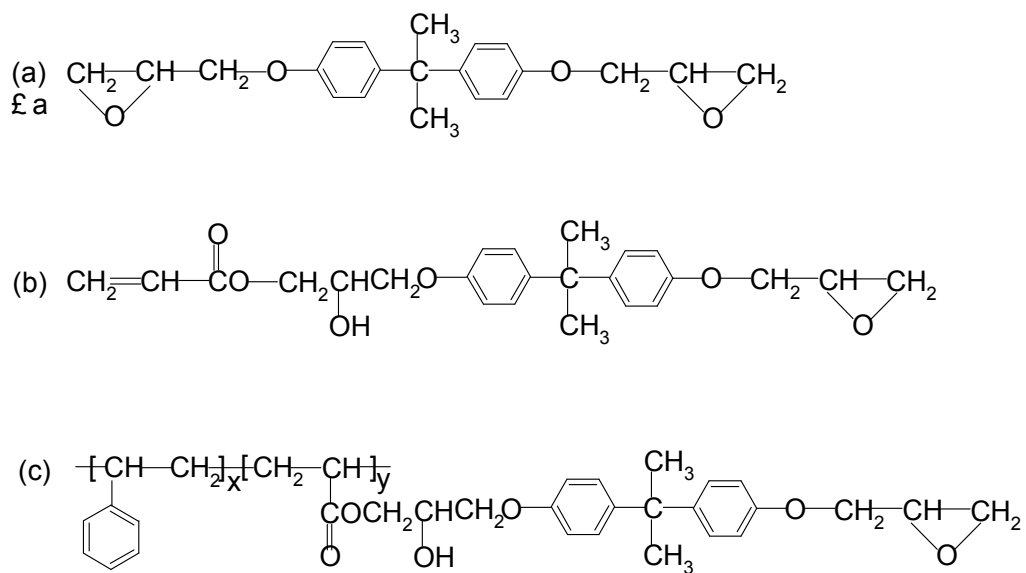


Fig. 2.  $^1\text{H}$  NMR spectra of (a) DGEBA (b) AADGEBA (c) PS-co-AADGEBA





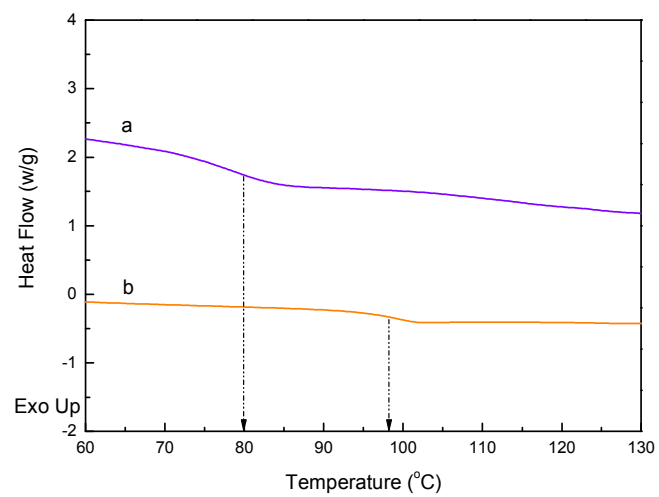


Fig. 3. DSC curves of (a) PS-co-AADGEBA (b) PS.

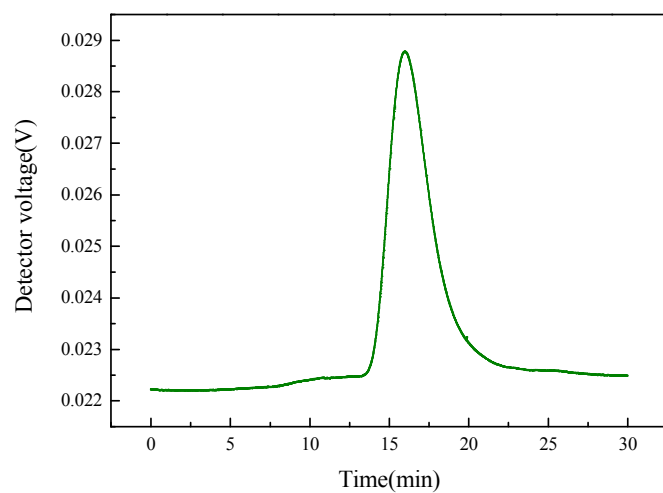


Fig. 4. GPC curves of PS-co-AADGEBAs.

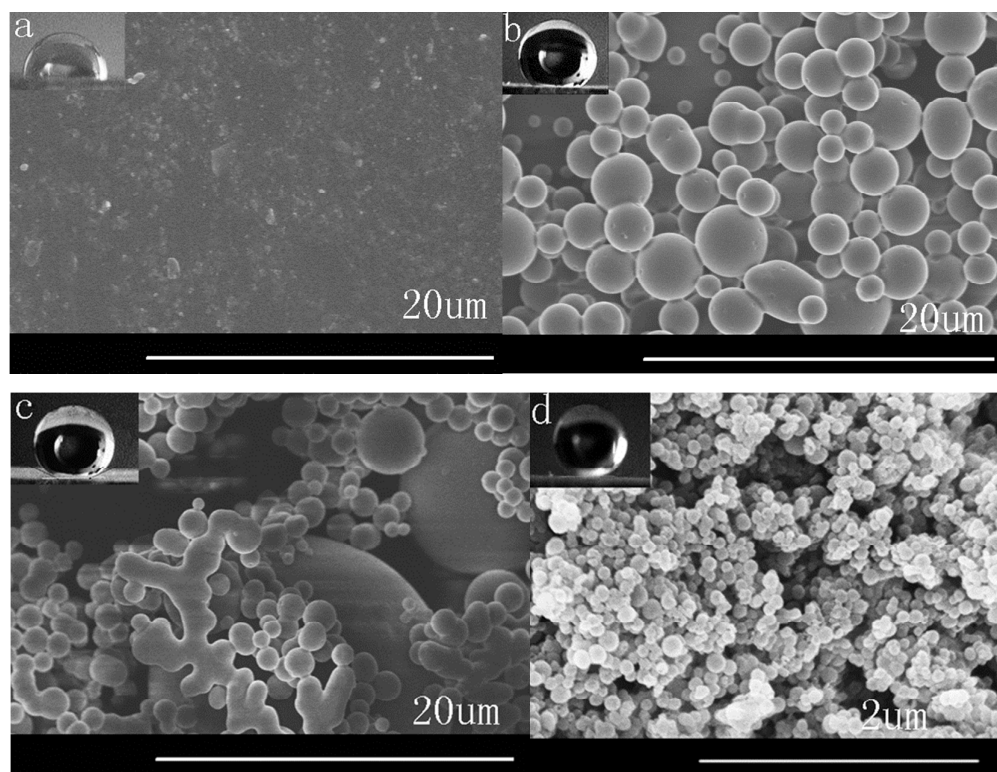


Fig. 5. SEM images of the PS-co-AADGEBA surface with different ethanol contents in the copolymer/THF solution: (a) 0%; (b) 30%; (c) 50%; (d) the (PS-co-AADGEBA)-g-(HSNs-NH<sub>2</sub>) surface.

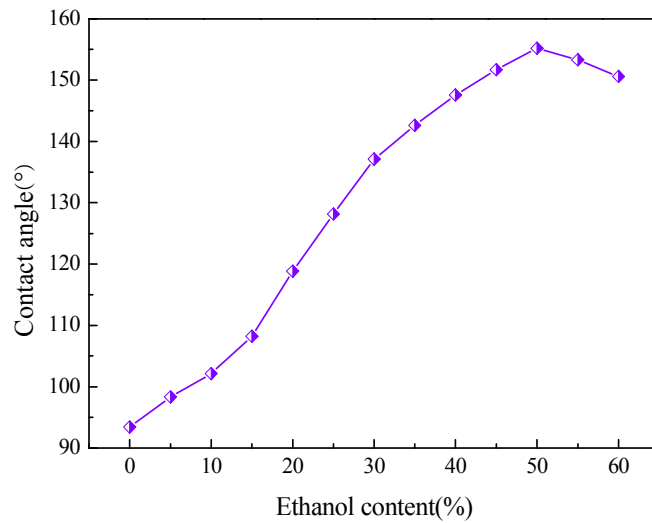


Fig. 6. The variation of water contact angles of the PS-co-AADGEBAs surface with different ethanol contents.

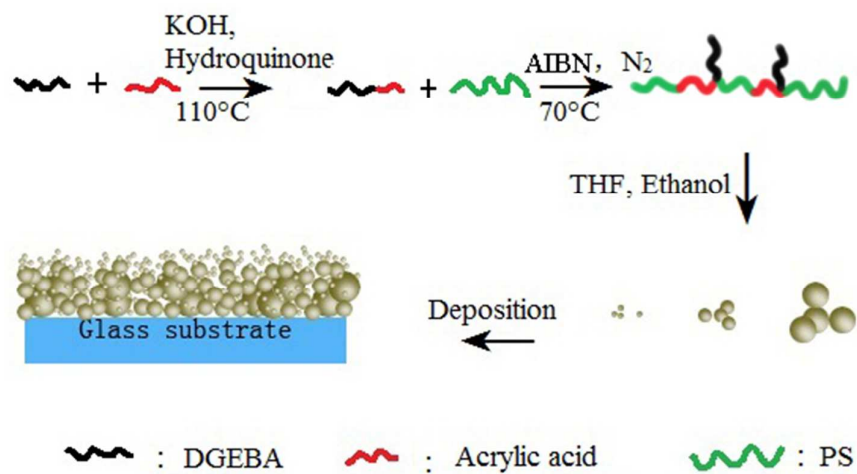


Fig. 7. Schematic diagram for the formation of the PS-co-AADGEBA surface.

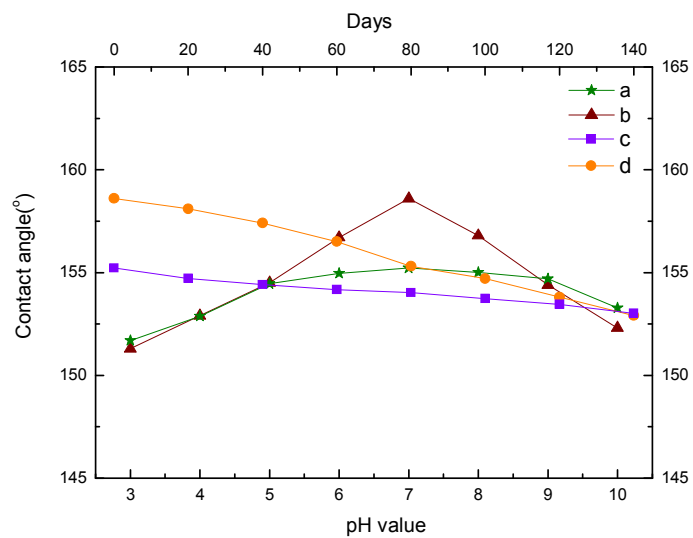


Fig. 8. CA as a function of pH value and exposure time for the PS-co-AADGEBA surface (a, c) and the (PS-co-AADGEBA)-g-(HSNs-NH<sub>2</sub>) surface (b, d), respectively.

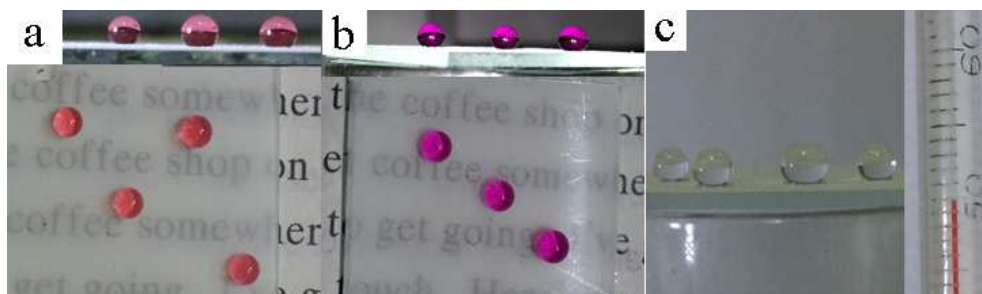


Fig. 9. Acid and alkali and hot water droplets on the PS-co-AADGEBA surface (a) acid droplets with methyl orange indicator (b) alkali droplets with phenolphthalein indicator (c) hot water of 50°C.

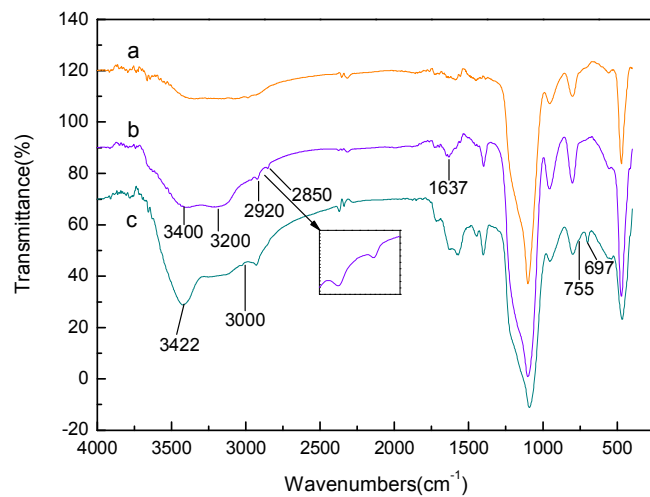


Fig. 10. FTIR spectra of (a) HSNs (b) HSNs-NH<sub>2</sub> (c) (PS-co-AADGEB A)-g-(HSNs-NH<sub>2</sub>).



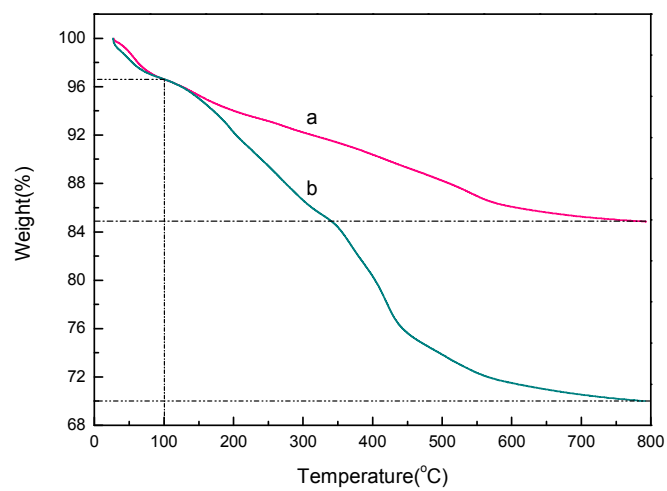
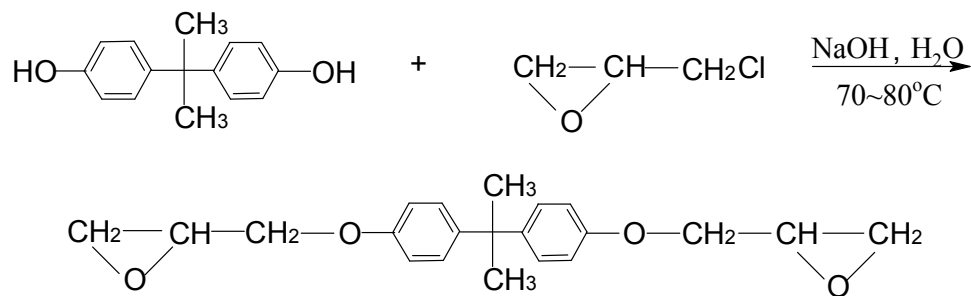
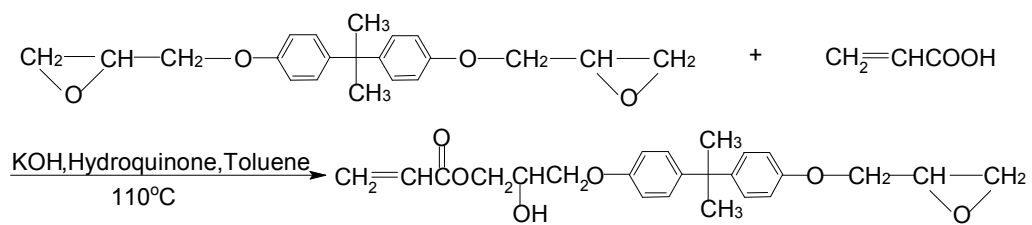


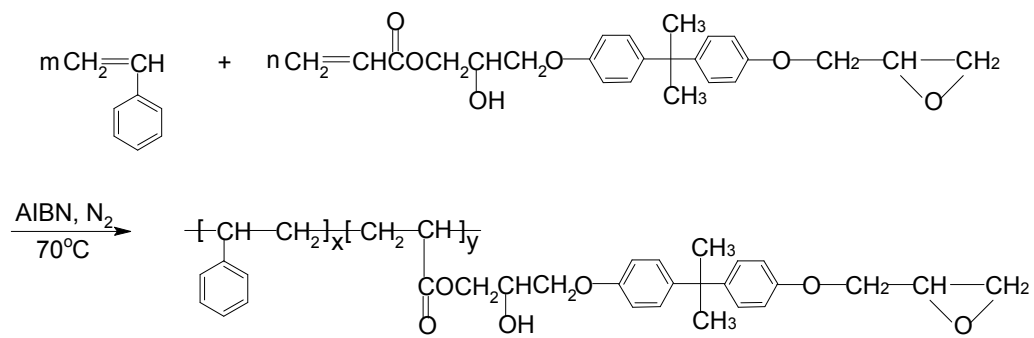
Fig. 11. TG curves of (a) HSNs-NH<sub>2</sub> (b) (PS-co-AADGEBa)-g-(HSNs-NH<sub>2</sub>).



**Scheme 1.** Synthesis of DGEBA.



**Scheme2.** Synthesis of AADGEBEA.



**Scheme 3.** Synthesis of PS-co-AADGEBAs.